RESEARCH ARTICLE

Hybrid polycaprolactone/hydrogel scaffold fabrication and in-process plasma treatment using PABS

Fengyuan Liu[1,†,*], Hussein Mishbak[1,2,†], Paulo Bartolo[1,*]

[1]Department of Science and Engineering, School of Mechanical, Aerospace and Civil Engineering, University of Manchester, Manchester, M13 9PL, UK
[2]Department of Biomedical Engineering, School of Engineering, University of Thi-Qar, Tai-Qar, Iraq

Abstract: A challenge for tissue engineering is to produce synthetic scaffolds of adequate chemical, physical, and biological cues effectively. Due to the hydrophobicity of the commonly used synthetic polymers, the printed scaffolds are limited in cell-seeding and proliferation efficiency. Furthermore, non-uniform cell distribution along the scaffolds with rare cell attachment in the core region is a common problem. There are no available commercial systems able to produce multi-type material and gradient scaffolds which could mimic the nature tissues. This paper describes a plasma-assisted bio-extrusion system (PABS) to overcome the above limitations and capable of producing functional-gradient scaffolds; it comprises pressure-assisted and screw-assisted extruders and plasma jets. A hybrid scaffold consisting of synthetic biopolymer and natural hybrid hydrogel alginate-gelatin (Alg-Gel) methacrylate anhydride, and full-layer N_2 plasma modification scaffolds were produced using PABS. Water contact angle and *in vitro* biological tests confirm that the plasma modification alters the hydrophilicity properties of synthetic polymers and promotes proliferation of cells, leading to homogeneous cell colonization. The results confirm the printing capability for soft hard material integration of PABS and suggest that it is promising for producing functional gradient scaffolds of biomaterials.

Keywords: Tissue engineering; hybrid scaffold; PABS; in-process plasma modification; functional gradient scaffold

[†]Co-first author, contributed equally to this work.

*Correspondence to: Paulo Bartolo, School of Mechanical, Aerospace and Civil Engineering, University of Manchester, Manchester, M13 9PL, UK; Email: paulojorge.bartolo@manchester.ac.uk

Fengyuan Liu, School of Mechanical, Aerospace and Civil Engineering, University of Manchester, Manchester, M13 9PL, UK; Email: fengyuan.liu@manchester.ac.uk

Received: November 27, 2018; **Accepted:** December 12, 2018; **Published Online:** December 31, 2018

Citation: Liu F, Mishbak H, Bartolo P. 2019 Hybrid polycaprolactone/hydrogel scaffold fabrication and in-process plasma treatment using PABS. Int J Bioprint, 5(1): 174. http://dx/doi.org/10.18063/ijb.v5i1.174

1. Introduction

Tissue engineering is promising for organ replacement which minimizes the side effects of organ transplantation[1,2]. Biomanufacturing is the major strategy of tissue engineering aiming at the development of biological substitutes that restore, maintain, or improve tissue function, and it requires the combined use of additive manufacturing (AM), biocompatible and biodegradable materials, cells, and biomolecular signals[3].

The scaffolds-based strategies (Figure 1) for tissue engineering have been most commonly used, depending strongly on materials and manufacturing processes. For materials, five types of biomaterials have been used: Acellular tissue matrices, synthetic polymers, natural polymers, ceramics, and polymer/ceramic composites[4-8]. The most commonly used biomaterial for producing scaffolds are synthetic polymers, such as polycaprolactone (PCL). Polymeric scaffolds play a pivotal role in tissue engineering through cell seeding, proliferation, and new tissue formation in three dimensions (3D), showing great promise in the research of engineering a variety of tissues. Moreover, scaffolds made from collagen are being rapidly replaced with ultraporous

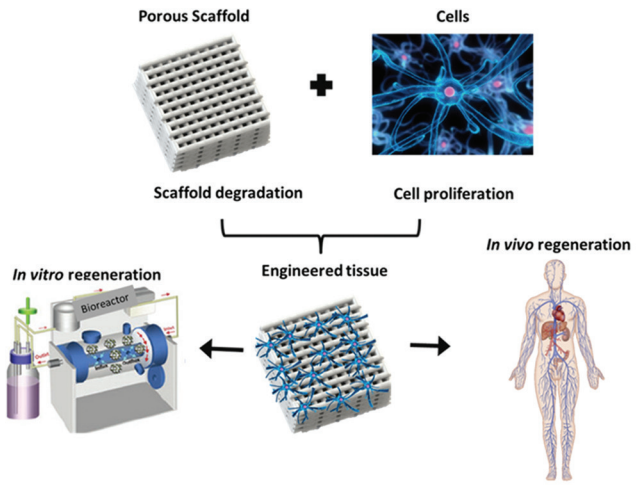

Figure 1. Scaffold-based approach for tissue engineering.

scaffolds from biodegradable polymers. Biodegradable polymers are attractive candidates for scaffolding materials because they degrade as the new tissues are formed, eventually leaving nothing foreign to the body. The major challenges in scaffold manufacturing lie in the design and fabrication of customizable biodegradable constructs with properties that promote cell adhesion and cell porosity, along with sufficient mechanical properties that match the host tissue, with predictable degradation rate and biocompatibility[9,10].

For the fabrication methods, AM techniques have been commonly applied in scaffold fabrication due to the superior ability in controlling pore size, pore shape, and pore distribution, and thus creating interconnected porous structures[3,11]. When combined with clinical imaging data, these fabrication techniques can be used to produce constructs that are customized to the shape of the defect or injury[12]. In terms of tissue and organ manufacturing, the additive nature ensures minimal waste of scarce and expensive building material, namely cells, growth factors, and biomaterials[13-15]. Among the AM techniques, material extrusion has been mostly applied in the bioengineering field due to the flexibility in material selection based on the use of pneumatic[16,17], piston[18], and screw-assisted[19-21] extrusion systems enabling a wider range of materials to be applied. Some processes operate at room temperature, thus allowing for cell encapsulation and biomolecule incorporation without significantly affecting viability. However, cell-seeding and proliferation efficiency is currently a big challenge due to the following limitations[22-25]:

- Most AM techniques are limited to single-material fabrication, which is difficult to provide an appropriate environment for cells due to the inadequate chemical, physical, and biological cues provided during AM processes.
- In addition, non-uniform cell distribution, especially rare cell adhesion in the core region of scaffolds, is often caused by the tortuosity of the constructs.
- Moreover, the synthetic biopolymers, most commonly used, are hydrophobic, and the cell colonization.

Different strategies have been explored to solve the above problems. Multi-material has been developed and utilized to produce multiple-material scaffolds [16,26]. However, most of these systems can only form one type of biomaterials, either soft hydrogels containing cells or bio-signals in the scale of KPa or rigid biopolymers and composites in the scale of MPa, which fails in the mimicry of natural tissues. In addition, low-temperature plasma modification is capable of improving the hydrophilicity of biopolymers by inducing certain functional groups on the surface to change the chemistry, wettability, and energy without altering the bulk properties[27,28]. However, most plasma treatment can be conducted after scaffolds printed and the penetration depth is limited, which results in non-uniform cell distribution along the scaffold.

A novel plasma-assisted bioprinting system (PABS) has been developed in the University of Manchester, allowing processing soft hard biomaterial integration and plasma surface modification layer by layer during the fabrication process in the same chamber. This paper utilized the plasma-assisted bio-extrusion system (PABS) to produce PCL/Hydrogel hybrid scaffolds and plasma fully treated scaffolds. The hydrogel is assessed with the preparation process, functionalization process, and rheology properties, while the PCL fully treated scaffolds are both morphologically and biologically assessed.

2. Materials and Methods

2.1. PCL

PCL (CAPATM6500, Mw = 50,000 g/mol), purchased from Perstorp (Cheshire, UK) in the form of 3 mm pellets, was used to produce the scaffolds. PCL is an easy-to-process semi-crystalline polymer with a density of 1.1 g/cm^3, a melting temperature between 58 and 60°C, and a glass transition temperature of -60°C.

2.2. Hybrid Hydrogel Methacrylate Anhydride (Alg-Gel) Ma Preparation

Hybrid hydrogel system platform was considered in this paper, which was made of mixing alginate methacrylate and gelation methacrylate at 50:50% v/v.

Functionalization process for both polymers (alginate and gelatin) is necessary to introduce the carbon-carbon double bond into the polymer chains that eventually convert the polymer into the photopolymerized polymer. According to published protocols[29], alginate was functionalized with methacrylate groups with minor modifications to be photopolymerized. The 2% wt. powder-type alginate (Sigma-Aldrich, UK) was

dissolved in Dulbecco's phosphate-buffered saline (DPBS) (Sigma-Aldrich, UK), and then mixed with MA (Sigma-Aldrich, UK) at 23% v/v of alginate solution under vigorous stirring. The pH of the solution was kept around 7.4 during the reaction time by the addition of 5M NaOH. The reaction time was 24 h. After the chemical modification, the polymer solution was precipitated with cold ethanol, dried in an oven overnight at 45°C and purified through dialysis for 6 days. The solution was then frozen at −80°C and recovered by lyophilization.

Gelatin was functionalized by dissolving gelatin bovine skin type B (Sigma-Aldrich, UK) at a concentration of 12.5%, in DPBS (Sigma-Aldrich, UK) at a temperature of 45°C. After gelatin dissolution, MA (×10 molar excess) was added under vigorous. The pH of the solution was kept around 7.0–8.0 during the reaction. The reaction time was 6 h. The solution was purified through dialysis for 7 days, frozen at −80°C and the polymer recovered by lyophilization.

2.3. Plasma-assisted Bio-extrusion System Set Up

Scaffolds were produces using a hybrid AM system called PABS, being developed at the University of Manchester. PABS (Figure 2A) comprises two main units, a multi-extrusion unit and a three-inlet plasma modification unit (Figure 2B). The multi-extrusion unit consists of two pressure-assisted extruders and one screw-assisted extruder, allowing operating a range of biomaterials, such as synthetic biopolymers, hydrogels, and biopolymer/ceramic composites. The extrusion unit has four movements: One rotational movement (C1) for selecting the required extrusion heads, a second rotational movement (C2) for driving and controlling the screw rotational speed of the screw-assisted extruder, and two linear movements (X and Y) in the X-Y plane. All these four movements are controlled by stepper motors and CNC drives. The build platform moves in the Z-direction and constitutes the sixth controllable axis. The build platform was fabricated using 7076 aluminum plate (250 mm × 200 mm × 7.5 mm) and is attached to the Z-axis rail guide with L-shape support underneath.

The plasma modification unit is mounted on the X-Y platform which is coplanar with the extrusion platform. Both platforms share common cylindrical guide rails in the X-direction. The Y-direction movement (V axis) for the plasma modification unit is independently driven by a stepper motor parallel to the Y-axis of the extrusion unit. A quartz capillary (outside diameter of 7 mm; inner diameter r of 5 mm; and length of 70 mm) with three gas inlets serves as the reaction jet. A tungsten rod (inner diameter of 2 mm) and one copper film (10 mm of width) wrapped around the quartz tube serve as the high-voltage and ground electrodes, respectively. The electrode is connected to a high-voltage DC power supply (applied voltage of 10 kV; frequency of 50 kHz). The plasma is generated from the top central electrode, expanding to the surrounding air inside and outside the nozzle.

The control system consists of a motion control system, temperature control system, and gas supply control system. The motion control system utilizes a Geo Brick LV motion controller (Delta Tau Data Systems, Inc) to manipulate all motors. The built-in software allows for complete machine logic control, including G code execution. The temperature control system consists of four digital temperature controllers (P.I.D. Omron E5CN), which is used to precisely control the temperature in the extruder heating chamber with polyimide thermos-foil heating elements (Omega Online/Kapton Heaters) and thermocouples (Omega). The gas supply control system includes an air compressor which works as the main gas supply, regulators, and gauges (SMC, UK), which enables pressure on/off control and manual adjustment. Power supply (230V ac, PHOENIX CONTACT) offers 24v output voltage and 40A current for all the control system. Safety considerations were taken into account regarding the electrical parts, including fuses, main circuit breakers, main filter, push buttons and estops (all supplied by OneCall Electronics Company, UK), and circuits. The control software was developed in MATLAB as previously reported and G code files were generated containing all the instructions for the fabrication process[30].

This configuration enables multi-material dispensing and plasma modification in a sequential mode. The system is able to achieve a maximum linear velocity of 20 mm/s and a resolution of 0.05 mm.

2.4. Scaffolds Printing Strategies

Scaffolds with a cross-section of 10 mm × 10 mm and a height of 3 mm were fabricated using the single laydown pattern of 0/90° and a filament distance of 1 mm with a pore size of 1 mm (slice thickness of 0.5 mm; heating temperature of 90°C; extrusion screw rotational speed of 15 rpm; and nozzle tip size of 0.5 mm.). The strategies for printing hybrid scaffolds and plasma treated scaffolds are as follows (Figure 3):

- Hybrid PCL/hydrogel scaffolds fabrication (Figure 3A): After the scaffold being printed with a screw-assisted extruder, the extruder selection unit rotated with 120°, and then the hydrogel solution was printed in the pores using the pressure-assisted extruder.
- Full-layer treated scaffolds fabrication (Figure 3B): The N_2 plasma modification was performed after one layer PCL was deposited, and the process was repeated until the last layer of PCL was complete. The treatment was conducted at a pressure of 0.689 bar and a flow rate of 5 L/mm. The deposition speed of the plasma jet was 3 mm/s, and each layer was subjected to the plasma treatment for 1 min. The

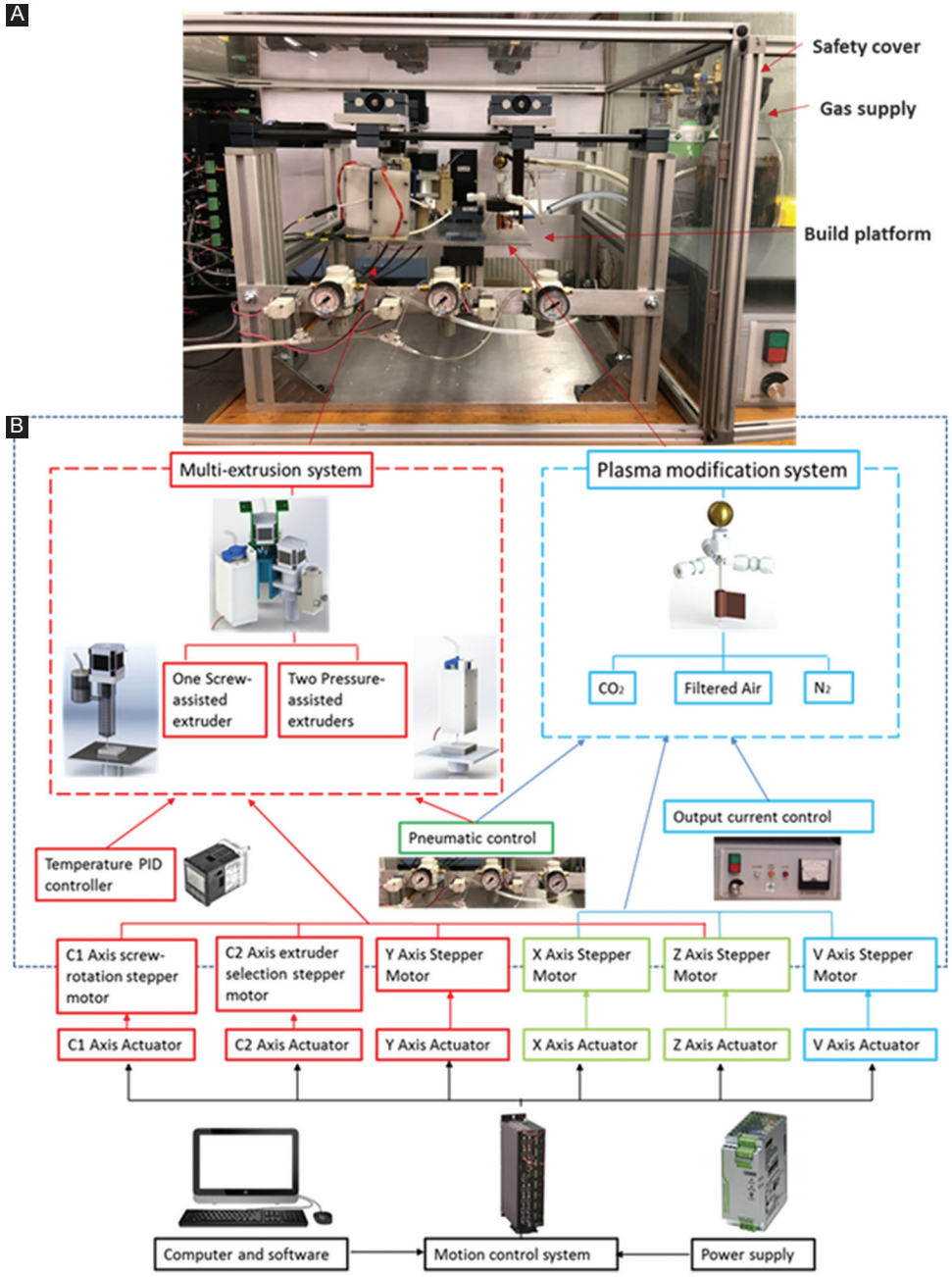

Figure 2. (A) Set-up of the plasma-assisted bio-extrusion system; (B) system diagram: Multi-extrusion system, plasma modification system, and control system.

distance from the bottom of the jet to the surface of the PCL filaments was 10 mm.

2.5. Morphology Characterization

Scanning electron microscopy (SEM) was used to assess the morphology and surface characteristic of printed scaffolds. The scaffolds were gold/palladium coated using a Q150T turbo-pumped sputter coater (Quorum technologies, UK) and imaged at 10 kV (Hitachi S3000N, Japan). These images were then analyzed using ImageJ software.

2.6. Wettability Measurement

Water contact angle (WCA) measurements on the flat surfaces of untreated and plasma-treated PCL scaffolds were carried out with a commercial KSV contact angle measuring 200 systems (KSV Instruments, Finland). The system is equipped with a CCD video camera and a micrometric liquid dispenser to drop 2 µL of distilled water on the surface of the scaffold. The measurements of the contact angles are automatically calculated with the instrument software.

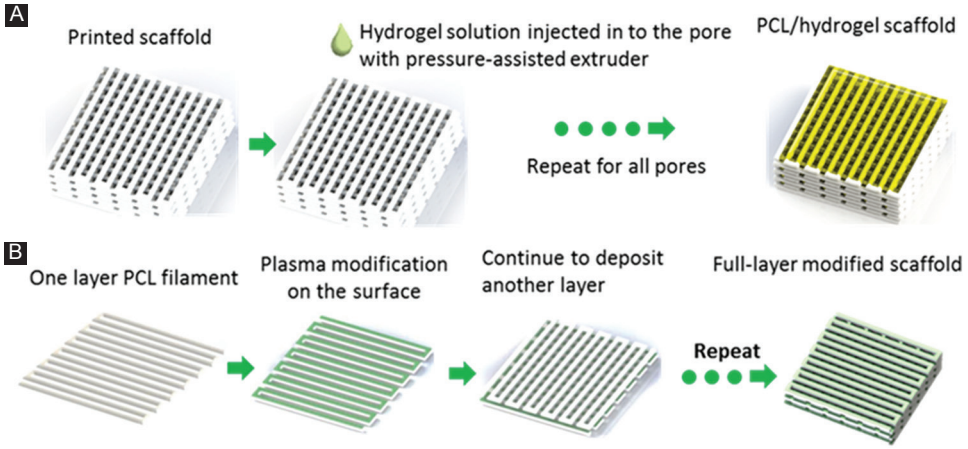

Figure 3. (A) Sequence of operations to fabricate hybrid polycaprolactone/hydrogel scaffolds; (B) sequence of operations to fabricate full-layer plasma-treated scaffolds.

2.7. Biological Tests

In vitro biological assessments were conducted with human adipose-derived stem cells (hADSCs) (STEMPRO, *in vitro* gen, Waltham, MA, USA). Before cell seeding, scaffolds were sterilized by soaking in 70% ethanol for 2 h. After sterilization, samples were rinsed twice in PBS (Gibco, Thermo Fisher Scientific, Waltham, MA, USA), transferred to 24-well plates and air-dried for 24 h at room temperature. 50,000 cells were seeded on each sample, including plasma-treated and untreated scaffolds.

Cell viability/proliferation behavior and the percentage of cells attached to the scaffolds (cell-seeding efficiency) were assessed through Alamar Blue assay (also termed the Resazurin assay, reagents from Sigma-Aldrich, UK). Cell viability/proliferation was measured at 1, 3, 7, and 14 days after cell seeding. For each measurement, cell-seeded scaffolds were transferred to a new 24-well plate, and 0.7 ml of Alamar Blue solution was added to each well, the plate was incubated for 4 h under standard condition (37°C, 5% CO_2, and 95% humidity). After incubation, 150 µL of each sample solution was transferred to a 96-well plate and the fluorescence intensity measured at 540 nm excitation wavelength and 590 nm emission wavelength with a spectrophotometer (Sunrise, Tecan, Männedorf, Zurich, Switzerland).

Cell attachment and distribution are assessed using laser confocal microscopy, with cell nuclei stained. At day 1 of cell culture and after 14 days, scaffolds were removed from 24-well cell culture plate, rinsed twice in PBS (Gibco, Thermo Fisher Scientific, Waltham, MA, USA), fixed with 10% neutral buffered formalin (Sigma-Aldrich, Dorset, UK) for 30 min at room temperature. After fixation, samples were rinsed twice with PBS for the removal of formalin, then permeabilized with 0.1% Triton-X100 (Sigma-Aldrich, Dorset, UK) in PBS at room temperature for 10 min, rinse twice for the removal of Triton-X100. Cell nuclei were stained blue by soaking scaffolds in a PBS solution containing 4′,6-Diamidine-2′-phenylindole dihydrochloride (Sigma-Aldrich, Dorset, UK) at the manufacturer recommended concentration. Samples were left in the staining solution for 10 min before removal, rinsed twice thoroughly with PBS. Confocal images were obtained using a 3D rendering mode on a Leica TCS SP5 (Leica, Milton Keynes, UK) confocal microscope, and cell colonization was quantified using a standard z-stack method. All images were taken at the center area of the scaffolds, and the experiments were performed three times in triplicate.

2.8. Data Analysis

All data are represented as mean ± standard deviation. Biological results were subjected to one-way analysis of variance (one-way) and *post hoc* Tukey's test using GraphPad Prism software. Significance levels were set at $P < 0.05$.

3. Results

3.1. Hybrid Scaffold Fabrication

The hybrid scaffold, consisting of PCL and hydrogel solution, was successfully fabricated using PABS. Figure 4A shows the image of the hybrid scaffold, where the porous structures hold the hydrogel solution without any deformation. Figure 4B and c present the top view and side view of the PCL/hydrogel scaffold, showing the position of the deposited hydrogel was precisely controlled and well adjacent with PCL scaffold.

3.2. Full-layer Treated PCL Scaffold

Figure 4B shows that the printed full-layer N_2 plasma treated scaffolds have a well-bonded interconnected

structure with a uniform pore distribution and pore size in the range of ~500 µm (Figure 4C). The N_2 plasma treatment was conducted at a pressure of 0.689 bar and a flow rate of 5 L/mm. The deposition speed of the plasma jet was 3 mm/s, and each layer was subjected to the plasma treatment for 1 min. The distance from the bottom of the jet to the surface of the PCL filaments was 10 mm. Figure 4D presents the filament surface after N_2 plasma modification, where lines in the direction of plasma movement can be observed making the surface roughness increased.

3.3. Wettability Assessment of Full-layer Plasma Modified Scaffold

WCA measurements were performed on untreated and fully treated plasma PCL scaffold surfaces to determine the effect of plasma modification on the surface wettability. Table 1 highlights the WCA results at different time points after the droplet was dropped on the surface of the scaffolds. The results show that in the case of an untreated PCL scaffold, there are no significant changes in the WCA values with time with values varying between 83.2±2.0° and 80.9±2.7°. For treated scaffolds, the WCA value, at 0 s, was lower (63.0±3.1°), leading to a fully wetting value of 26.7±0.9° at 0.5 s. At 3 s, the droplet was fully absorbed

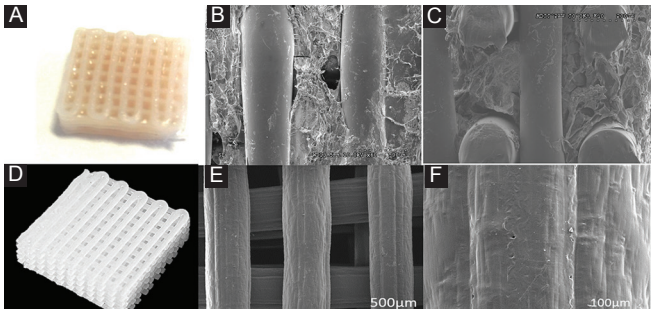

Figure 4. (A) Hybrid polycaprolactone (PCL)/hydrogel scaffold; (B) Scanning electron microscopy (SEM) image of top view of PCL/hydrogel scaffold; (C) SEM image of side view of PCL/hydrogel scaffold; (D) photo of a full-layer N_2 plasma-treated PCL scaffold; (E) SEM image of top view of full-layer N_2 plasma treated PCL scaffold; (F) SEM image of filament surface of full-layer N_2 plasma-treated PCL scaffold.

Table 1. Temporal variation of WCAs for treated and untreated scaffolds

Time	PCL scaffolds	N_2 plasma fully treated
0s	83.2±2.0°	63.0±3.1°
0.5s	82.9±1.2°	26.7±0.9°
3s	80.9±2.7°	Fully absorbed

PCL: Polycaprolactone, WCAs: Water contact angles

3.4. Biological Assessment of Full-layer Plasma Modified Scaffold

The adhesion and proliferation of hADSCs cells on plasma full-layer modified PCL scaffolds were studied and compared with untreated ones. The biological characterization was assessed using Alamar Blue Assay. The fluorescence intensity of cell-seeded scaffolds measured at four different culture time points (Days 1, 3, 7, and 14) is shown in Figure 5A. Higher fluorescence intensity corresponds to more metabolically active cells. As observed, cell proliferation increases with time in all types of scaffolds, suggesting that they are suitable structures for cell attachment and proliferation. However, a fast proliferation rate is observed in the case of plasma-treated scaffolds. The different performance is statistically significant after day 3.

Confocal microscopy images (Figure 5B) present the cell attachment and distribution after cell seeding (day 1) and proliferation (day 14). It can be observed that plasma-treated scaffolds presented higher numbers of cells than untreated scaffolds. In addition, it is also possible to observe that the plasma surface-treated scaffolds presented best cell attachment and dispersion.

4. Discussion

The printed hybrid PCL scaffolds filled with hydrogel present the printability of PBAS, enabling the soft hard material integration. The photo and SEM images of the whole printed structure indicate that the plasma modification process does not affect the physical appearance of the structure and potentially no effect on the mechanical performances[31]. Moreover, the SEM image of the filament surface confirms the increased surface roughness is due to the etching process[32], which results in the stripping off the topmost layer of the polymer filament. From this study, the increase surface roughness is also resulted from the linear scratches attributed to the gas flow by the plasma jetting directly after the PCL deposition when the material is still in the molten status. As the printed material is not totally cooled down, when the plasma modification occurs, the gas flow effect is stronger, significantly influencing the surface topography. Moreover, the increase of surface roughness is beneficial for cell colonization in the scaffolds[33].

The wettability results reveal that the hydrophilicity of the surface is dramatically improved due to the ionizable groups introduced on the surface by the N_2 plasma, which enhances the hydrogel bonding with water. Compared with the results published in[28,34], the absorption speed is dramatically increased, due to chemical heterogeneity on the surface of each layer due to the plasma modification layer on layer. However, the effect of plasma modification can last within a certain period of time depending

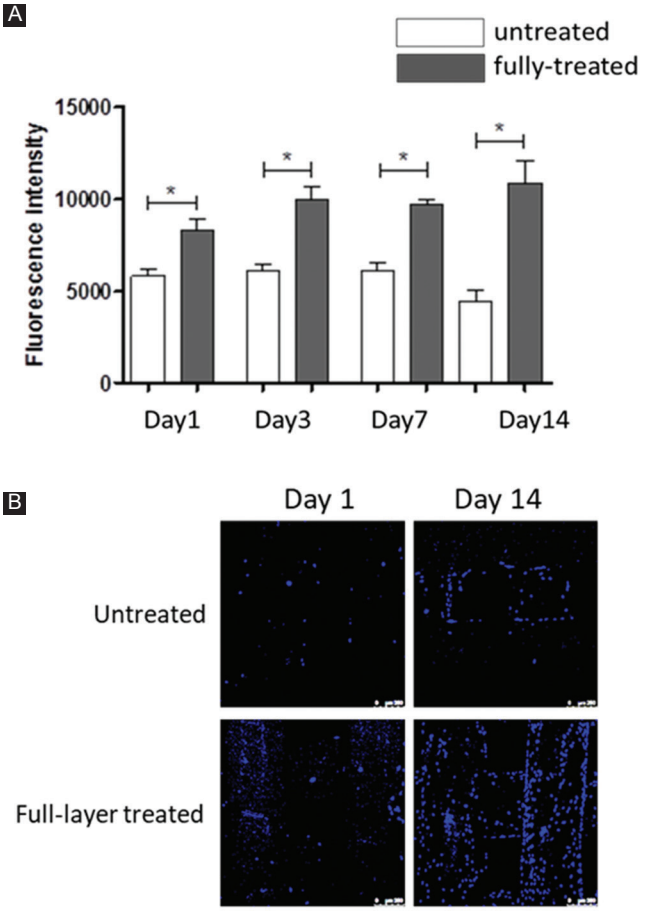

Figure 5. (A) Temporal variation of fluorescence intensity of cell-seeded PCL scaffolds with and without N_2 plasma treatment; (B) confocal microscope images of untreated and full-layer treated of cell-seeded scaffolds, 1 day and 14 days after cell culture. Scale bar 250 μm.

on the density of chemical reagents deposited on the surface, and the effect also decreases with time since the structural rearrangement of polymer chains resulting in the decreased surface energy[35].

In addition, it is important to control hydrogels printability window (injection, deposition, and extrusion) during the printing process to mimic the native organ structures. To achieve precise printable properties, hydrogels have been designed to achieve adjustable viscoelastic behavior, and the SEM images confirm the liquid-like-gel structure before printing and quick gelation kinetics to produce a structure with good fidelity.

4.1. This Makes it Easy to Inject Hybrid Hydrogel System (Alg-Gel) MA

Consistent with the other studies[36,37], a significant increase in the biological behavior is observed after plasma modification. Since the hydrophilicity has been improved with the plasma modification process, the environment is changed to be more suitable for cell colonization and proliferation. Furthermore, with the full-layer plasma modification capability, the plasma active species can reach the walls of the pores on each layer of the scaffold, leading to the uniform cell distribution along the scaffold. This will enable a higher rate of tissue formation in the clinical research.

5. Conclusion

This paper presents a novel AM system comprising a multi-material printing unit and a plasma jet unit. To assess the system, hybrid PCL/hydrogel scaffolds and full-layer plasma treated PCL scaffolds were produced. The effect of plasma treatment on PCL samples was examined. WCA results confirmed that the hydrophilic character of the PCL samples increased due to the nitrogen groups introduced by the plasma jetting on the scaffold filaments. It was also possible to observe that the plasma treatment positively influences cell attachment and proliferation. Applications that may benefit from this technology include hybrid tissue, which has compositional variations depending on the region or organ-like structure that require the continuous vascular network to facilitate nutrient diffusion.

Acknowledgments

The authors wish to acknowledge the support from the School of Mechanical, Aerospace and Civil Engineering at the University of Manchester.

Conflicts of Interest

The authors declare that they have no conflicts of interest.

References

1. Pereira R F, Sousa A, Barrias C C, *et al.*, 2017, Advances in bioprinted cell-laden hydrogels for skin tissue engineering. *Biomanuf Rev*, 2(1): 1. https://doi.org/10.1007/s40898-017-0003-8.
2. Melchels F P, Domingos M A, Klein T J, *et al.*, 2012, Additive manufacturing of tissues and organs. *Prog Polym Sci*, 37(8): 1079-1104. https://doi.org/10.1016/j.progpolymsci.2011.11.007.
3. Vyas C, Pereira R, Huang B, *et al.*, 2017, Engineering the vasculature with additive manufacturing. *Curr Opin Biomed Eng*, 2: 1-13. https://doi.org/10.1016/j.cobme.2017.05.008.
4. Rahman S, Carter P, Bhattarai N, 2017, *Aloe vera* for tissue engineering applications. *J Funct Biomater*, 8(1): 6. https://doi.org/10.3390/jfb8010006.
5. Maldonado M A, Bonham A J, 2017, Conductive gel polymers as an extracellular matrix mimic and cell vehicle for cardiac tissue engineering. *FASEB J*, 31(1_supplement):

925.921-925.921.

6. Black C R, Goriainov V, Gibbs D*, et al.*, 2015, Bone tissue engineering. *Curr Mol Biol Rep*, 1(3): 132-140. https://doi.org/10.1007/s40610-015-0022-2.
7. Asghari F, Samiei M, Adibkia K*, et al.*, 2017, Biodegradable and biocompatible polymers for tissue engineering application: A review. *Artif Cells Nanomed Biotechnol*, 45(2): 185-192. https://doi.org/10.3109/21691401.2016.1146731.
8. Trombetta R, Inzana J A, Schwarz E M*, et al.*, 2017, 3D printing of calcium phosphate ceramics for bone tissue engineering and drug delivery. *Ann Biomed Eng*, 45(1): 23-44. https://doi.org/10.1007/s10439-016-1678-3.
9. Vacanti J P, Langer R, 1999, Tissue engineering: The design and fabrication of living replacement devices for surgical reconstruction and transplantation. *Lancet*, 354: S32-S34. https://doi.org/10.1016/S0140-6736(99)90247-7.
10. Mohanty A K, Misra M, Hinrichsen G, 2000, Biofibres, biodegradable polymers and biocomposites: An overview. *Macromol Mater Eng,* 276(1): 1-24. https://doi.org/10.1002/(SICI)1439-2054(20000301)276:1<1::AID-MAME1>3.0.CO;2-W.
11. Kumar A, Mandal S, Barui S*, et al.*, 2016, Low temperature additive manufacturing of three dimensional scaffolds for bone-tissue engineering applications: Processing related challenges and property assessment. *Mater Sci Eng Rep*, 103: 1-39. https://doi.org/10.1016/j.mser.2016.01.001.
12. Forrestal D P, Klein T J, Woodruff M A, 2017, Challenges in engineering large customized bone constructs. *Biotechnol Bioeng*, 114(6): 1129-1139. https://doi.org/10.1002/bit.26222.
13. Bártolo P, Chua C, Almeida H*, et al.*, 2009, Biomanufacturing for tissue engineering: Present and future trends. *Virtual Phys Prototyp*, 4(4): 203-216. https://doi.org/10.1080/17452750903476288.
14. Bártolo P J, Domingos M, Patrício T*, et al.*, 2011, Biofabrication strategies for tissue engineering. *Adv Model Tissue Eng,* 11: 137-176. https://doi.org/10.1007/978-94-007-1254-6_8.
15. Bartolo P, Kruth J P, Silva J*, et al.*, 2012, Biomedical production of implants by additive electro-chemical and physical processes. *CIRP Ann Manuf Technol*, 61(2): 635-655. https://doi.org/10.1016/j.cirp.2012.05.005.
16. Rutz A L, Hyland K E, Jakus A E*, et al.*, 2015, A multimaterial bioink method for 3D printing tunable, cell-compatible hydrogels. *Adv Mater*, 27(9): 1607-1614. https://doi.org/10.1002/adma.201405076.
17. Jakus A E, Shah R N, 2017, Multi and mixed 3D-printing of graphene-hydroxyapatite hybrid materials for complex tissue engineering. *J Biomed Mater Res Part A*, 105(1): 274-283. https://doi.org/10.1002/jbm.a.35684.
18. Hoque M E, Chuan Y L, Pashby I, 2012, Extrusion based rapid prototyping technique: An advanced platform for tissue engineering scaffold fabrication. *Biopolymers*, 97(2): 83-93.
19. Bellini A, 2002, *Fused Deposition of Ceramics: A Comprehensive Experimental, Analytical and Computational Study of Material Behavior, Fabrication Process and equipment Desig*. Philadelphia, PA: Drexel Universityn.
20. Almeida H, Bartolo P, Mota C, *et al*., 2010, Process equipment for rapid bioextrusion fabrication. *Portuguese Patent Appl*, 104, 247.
21. Zhang L G, Fisher J P, Leong K, 2015, *3D Bioprinting and Nanotechnology in Tissue Engineering and Regenerative Medicine*. London: Academic Press.
22. Giannitelli S, Mozetic P, Trombetta M*, et al.*, 2015, Combined additive manufacturing approaches in tissue engineering. *Acta Biomater*, 24: 1-11. https://doi.org/10.1016/j.actbio.2015.06.032.
23. Sobral J M, Caridade S G, Sousa R A*, et al.*, 2011, Three-dimensional plotted scaffolds with controlled pore size gradients: Effect of scaffold geometry on mechanical performance and cell seeding efficiency. *Acta Biomater*, 7(3): 1009-1018. https://doi.org/10.1016/j.actbio.2010.11.003.
24. Oh S H, Lee J H, 2013, Hydrophilization of synthetic biodegradable polymer scaffolds for improved cell/tissue compatibility. *Biomed Mater*, 8(1): 014101. https://doi.org/10.1088/1748-6041/8/1/014101.
25. Yang J, Wan Y, Yang J*, et al.*, 2003, Plasma-treated, collagen-anchored polylactone: Its cell affinity evaluation under shear or shear-free conditions. *J Biomed Mater Res Part A*, 67(4): 1139-1147. https://doi.org/10.1002/jbm.a.10034.
26. Ozbolat I T, Chen H, Yu Y, 2014, Development of 'multi-arm bioprinter' for hybrid biofabrication of tissue engineering constructs. *Robot Comput Integr Manuf*, 30(3): 295-304. https://doi.org/10.1016/j.rcim.2013.10.005.
27. Intranuovo F, Gristina R, Brun F*, et al.*, 2014, Plasma modification of PCL porous scaffolds fabricated by solvent-casting/particulate-leaching for tissue engineering. *Plasma Process Polym*, 11(2): 184-195. https://doi.org/10.1002/ppap.201300149.
28. Intranuovo F, Gristina R, Fracassi L*, et al.*, 2016, Plasma processing of scaffolds for tissue engineering and regenerative medicine. *Plasma Chem Plasma Process*, 36(1): 269-280. https://doi.org/10.1007/s11090-015-9667-0.
29. Jeon O, Bouhadir K H, Mansour J M*, et al.*, 2009, Photocrosslinked alginate hydrogels with tunable biodegradation

rates and mechanical properties. *Biomaterials*, 30(14): 2724-2734. https://doi.org/10.1016/j.biomaterials.2009.01.034.

30. Liu F, Hinduja S, Bartolo P, 2018, User interface tool for a novel plasma-assisted bio-additive extrusion system. *Rapid Prototyp,* 10: 1108.https://doi.org/10.1108/RPJ-07-2016-0115.
31. Park K, Ju Y M, Son J S*, et al.*, 2007, Surface modification of biodegradable electrospun nanofiber scaffolds and their interaction with fibroblasts. *J Biomater Sci Polym* , 18(4): 369-382. https://doi.org/10.1163/156856207780424997.
32. Thakur S, Neogi S, 2015, Tailoring the adhesion of polymers using plasma for biomedical applications: A critical review. *Rev Adhes Adhes*, 3(1): 53-97. https://doi.org/10.7569/RAA.2015.097303.
33. Gross M, Zhao X, Mascarenhas V*, et al.*, 2016, Effects of the surface physico-chemical properties and the surface textures on the initial colonization and the attached growth in algal biofilm. *Biotechnol Biofuel*, 9(1): 38. https://doi.org/10.1186/s13068-016-0451-z.
34. Hashimoto M, Hossain S, Masumura S, 1999, Effect of aging on plasma membrane fluidity of rat aortic endothelial cells-.☆ *Exp Gerontol*, 34(5): 687-698. https://doi.org/10.1016/S0531-5565(99)00025-X.
35. Wavhal D S, Fisher E R, 2002, Hydrophilic modification of polyethersulfone membranes by low temperature plasma-induced graft polymerization. *J Membr Sci*, 209(1): 255-269. https://doi.org/10.1016/S0376-7388(02)00352-6.
36. Pappa A M, Karagkiozaki V, Krol S*, et al.*, 2015, Oxygen-plasma-modified biomimetic nanofibrous scaffolds for enhanced compatibility of cardiovascular implants. *Beilstein J Nanotechnol*, 6: 254. https://doi.org/10.3762/bjnano.6.24.
37. Sousa I, Mendes A, Pereira R F*, et al.*, 2014, Collagen surface modified poly (ε-caprolactone) scaffolds with improved hydrophilicity and cell adhesion properties. *Mater Lett*, 134: 263-267. https://doi.org/10.1016/j.matlet.2014.06.132.